ICES Journal of Marine Science, 2026, Vol. 83, Issue 2, fsag020
https://doi.org/10.1093/icesjms/fsag020
Original Article

Despite temperature effects on gonad development, timing of spawning is remarkably flexible in Atlantic cod

Anders Frugård Opdal [1,*], Maud Alix[2], Olav Sigurd Kjesbu [2], Christian Jørgensen [1], Øystein Langangen [3], Ørjan Karlsen [2], Kate McQueen [2], Daniel Nyqvist[4], Esben Moland Olsen[5], Anders Thorsen[2], Jon Egil Skjæraasen[2]

[1]University of Bergen, Department of Biological Sciences, Thormøhlens gate 53A, 5006 Bergen, Norway
[2]Institute of Marine Research, Nordnesgaten 50, 5005 Bergen, Norway
[3]University of Oslo, Department of Biosciences, Blindernveien 31, 0371 Oslo, Norway
[4]Swedish University of Agricultural Sciences, Department of Aquatic Resources, Almas allé 8, 756 51 Uppsala, Sweden
[5]Institute of Marine Research, Flødevigen Research Station, Nye Flødevigveien 20, 4817 His, Norway
*Corresponding author. University of Bergen, Department of Biological Sciences, Thormøhlens gate 53A, 5006 Bergen, Norway. E-mail: anders.opdal@uib.no.

Abstract

At high latitudes, early life stage survival of fish is often associated with how spawning time relates to the timing of the spring bloom. With ocean warming, basic physiological rates of ectotherms, like fish, will speed up—including gonadal development rates, which dictate spawning time. Since warmer water is thought to influence the spring bloom timing differently than that of fish spawning time, the two may fall out of synchrony in the future. The precise mechanisms between temperature and gonadal development and spawning time have, however, been difficult to disentangle. Here, we take advantage of a series of independent laboratory experiments measuring individual oocyte development up to or near spawning for 153 Atlantic cod (*Gadus morhua*) kept between 3 and 12°C. From these data we derive a predictive, mechanistic equation for daily oocyte growth rate as a function of temperature and oocyte developmental status (diameter). The vitellogenic oocyte growth follows an accelerating pattern, and the model predicts that spawning can advance by up to 7 days per 1°C increase. Within-treatment variation is, however, of comparable magnitude to between-treatment temperature effects. The model was also tested in the field by back-calculating oocyte development of 82 fish (2018–2021) sampled at two locations along the Norwegian coast, using daily ambient temperatures from telemetry tags during vitellogenesis as model input. We find that Atlantic cod are able to initiate vitellogenesis over a period of several months in late summer and autumn, as well as regulate the oocyte development rate across a wide range of temperatures—both leading to significant phenotypic plasticity in spawning phenology.

Keywords *Gadus morhua*, phenology, spawning, oocyte, physiology, climate change, telemetry, trophic asynchrony, match-mismatch

Introduction

At high latitudes, strong seasonality influences most aspects of life. Little light and low temperatures in winter severely constrain primary production and biological rates, which have given rise to a series of life history strategies for enduring winter in anticipation of better times. In the ocean, we refer to these systems as spring-bloom ecosystems (Sverdrup et al. 1942, Longhurst 2007), as the nutrients that build up slowly over winter fuel a rapid phytoplankton bloom in spring, providing an annual rhythm that various types of organisms are attuned to.

Many species of fish and zooplankton in these waters reproduce during the winter-spring transition, as it provides offspring with abundant food for fast growth and high survival, but also ample time for developing and preparing for the next winter (Qasim 1956, Cushing 1969, Melle et al. 2014). There are good reasons to agree with Hjort's (1914) classical focus on how offspring survival is likely highest when there is maximal spatiotemporal overlap between first-feeding fish larvae and their zooplankton prey (Hjort 1914, Cushing 1990).

A key question is, however, to what degree adult fish have the capability to sense the relevant environment and flexibly adjust the timing of spawning to maximize overlap between food and first-feeding. One extreme answer is underscored in Cushing's original formulation of the match-mismatch hypothesis (Cushing 1973), where a central assumption was that fish in temperate regions, including Atlantic cod, spawn at more or less regular times in spring (Cushing 1969). Such a view implies that fish have restricted flexibility, and that recruitment success primarily reflects luck, good or bad, as external influences instead affect the timing of larval food availability. A similar argument is that the best spawning time is so variable and noisy that fish just sample a broad set of possible outcomes, i.e. bet-hedging, as e.g. Atlantic cod that spawn several batches 3–4 days apart (Meek 1911); up

Received: 10 November 2025. **Revised:** 30 January 2026. **Accepted:** 30 January 2026

to 19 batches have been recorded over up to 6 weeks (Kjesbu 1989).

Both these types of fixed strategies imply that a large fraction of the investment in reproduction may be fruitless due to mismatch between fish larvae and their food. In contrast, a range of studies have shown that spawning time can be highly variable between years (Opdal et al. 2024a, Pedersen 1984, Hutchings and Myers 1994, Wieland et al. 2000, Fincham et al. 2013, Morgan et al. 2013) and perhaps even phenotypically flexible (Opdal et al. 2024a, Opdal et al. 2024b)—a possibility that was also briefly mentioned by Cushing (1969). It then matters how the phenotypic trait of spawning phenology is expressed, since physiological rates may be determined or constrained by temperature, whereas behavioural traits may incorporate further environmental cues and thus add flexibility.

Both laboratory and field studies have shown that with increasing temperatures, the developmental rates of gonads increase (Ware and Tanasichuk 1989, Kjesbu et al. 2010), thus advancing the timing of spawning (Poloczanska et al. 2016, McQueen and Marshall 2017, Neuheimer et al. 2018, Rogers and Dougherty 2019, Tanaka et al. 2019). Such physiological determinism has raised concerns because it implies that spawning takes place earlier as the ocean warms, possibly out of sync with prey availability. The most recent literature is reviewed in the latest IPCC report (AR6 WG2), which concluded that at 'latitudes $>$ 40°N, temperature-linked phenology of fish reproduction with high geographic fidelity to spawning grounds (geographic spawners) is projected to change at double the rate of that for phytoplankton, which will likely cause phenological mismatches resulting in increased risk of starvation for fish larvae (medium to high confidence)' (Cooley et al. 2022, p. 437).

Given the potentially futile reproductive costs of a fixed spawning strategy, one could logically expect that the cumulative phenological uncertainty propagating through trophic levels from ocean physics via phytoplankton and zooplankton through to larval fish would exert strong selection pressures towards mechanisms that allow careful timing of fish spawning. Consequently, there are reasons to expect that adaptations capable of somehow directing effort towards the best spawning times have evolved, i.e. the ability to adjust spawning time beyond the temperature-driven rates of gonad development (Opdal et al. 2024b). Such flexibility, arising from physiological or behavioural degrees of freedom, will complement and extend earlier hypotheses that cod start vitellogenesis within a restricted time window, from which spawning time is nearly physiologically determined based on Arrhenius, Q_{10} (e.g. Witthames and Greer Walker 1995, Kjesbu et al. 2010) or degree-day (Neuheimer et al. 2018) principles.

Here we consolidate these views by analysing how temperature affects gonad development while also explicitly including the role of individual variation. This broadened perspective is quite different from earlier studies investigating temperature effects on spawning time, which were all based on averaged effects (Kjesbu et al. 2010, Pankhurst and Munday 2011, Neuheimer and MacKenzie 2014, McQueen and Marshall 2017, Neuheimer et al. 2018, Rogers and Dougherty 2019).

This study involves a combination of temperature-controlled experiments, field observations, and climate projections. In short, we used experimental individually resolved data from Atlantic cod (*Gadus morhua*) to derive a model for daily vitellogenic oocyte growth as a function of oocyte diameter and temperature. We then confronted this laboratory-derived statistical model with field data by using field observations of vitellogenic temperature trajectories to predict oocyte size and comparing these with oocytes sampled in the field. This approach allowed us to construct a state–of–the–art, temperature–based model for cod oocyte growth that incorporates individual plasticity, hopefully providing a more accurate representation of cod phenology in a warmer ocean.

Materials and methods

All methods relating to animal experiments were carried out in accordance with the ARRIVE guidelines, an international checklist for transparent reporting of animal research (https://arriveguidelines.org). Permission to conduct this research at the Institute of Marine Research (IMR), Norway, was given by the Norwegian Animal Research Authority.

We first analysed data from multiple temperature experiments with statistical methods that make use of repeated observations of the same individuals. Our approach thus propagates individual variation in how temperature affects oocyte developmental rates and estimates confidence intervals for a population of spawning females.

The statistical model was then rigorously tested against field data from sexually mature cod tagged with telemetry tags at two locations along the Norwegian coast. For these cod, ambient *in situ* temperature exposure was recorded every few minutes throughout the several months of oocyte development. Of particular interest are two individual females for which oocyte size was measured from histology at recapture just prior to spawning, plus they had carried loggers that yielded experienced trajectories of temperature for the entire vitellogenic period. These two females and a broader cross-sectional dataset on experienced temperature and oocyte size allow us to use the laboratory-derived model to estimate oocyte size and compare these to measurements of actual oocyte size obtained in the field prior to spawning.

Temperature-controlled tank experiments of oocyte development

Our study utilized results from two different temperature-controlled experiments, the first (Experiment 1) conducted in 2005–2006 (at 5 and 9.6°C) and the second (Experiment 2) in 2018–2019 (at 3, 6, 9, and 12°C); further details on the methodology are published in Kjesbu et al. (2010) and Skjærven et al. (2024), respectively.

Experiment 1 took place at the facilities of Institute of Marine Research (IMR) in Bergen between 1 June 2005 (as 2-year-olds) and 26 January 2006 (as 3-year-olds). Fish were supplied from a local rearing facility operated by the IMR in the Parisvatnet marine pond west of Bergen (60.6°N, 4.8°E), after which they were kept at IMR Austevoll Research Station for further on-growth. In spring 2005, 155 fish, males and females, were divided into two outdoor 30 m^3 tanks with natural seawater (inlets at 50 and 120 m depth). The initial mean length and weight [95% CI] of females ($N = 71$) were 60.2 [59.2, 61.2] cm and 2.96 [2.8, 3.1] kg with a range of 43.5 to 68.0 cm and 1.7 to 4.0 kg, respectively. Starting 1 June, fish were randomly re-distributed between tanks. One tank remained at ambient seawater temperatures (average of 9.6°C over the study period), while

the other tank was gradually cooled overnight to 5°C, a temperature maintained for the rest of the experiment.

Experiment 2 took place at the IMR Matre Research Station (north of Bergen) between 1 October 2018 and 26 April 2019. A total of 200 coastal cod were wild-caught with eel nets outside the island Bømlo, south of Bergen (59.8°N, 5.3°E), continuously over an extended period, starting in spring and continuing until about one month prior to transportation. While awaiting transport to Matre in early September, they were kept in sea cages holding ambient temperatures between 4 and 17°C (based on temperatures at 5 m depth in Austevoll between March and August 2018). The initial mean total length and weight [95% CI] of females ($N = 141$) were 65.6 [63.4, 67.8] cm and 3.8 [3.5, 4.1] kg with a range of 43.5 to 90.0 cm and 1.2 to 8.0 kg, respectively. In Matre, the fish were randomly and evenly distributed into twelve 8 m^3 indoor tanks (14 to 18 fish per tank) with natural, filtered seawater at 8°C (inlet at 90 m depth). Light was programmed to follow the natural photoperiod at 60.0°N. Starting on 1 October, temperatures in the tanks were adjusted at a maximum of 1°C per day (heated or cooled as needed) until they reached 3, 6, 9, and 12°C (3 tanks per temperature).

All tanks in both experiments had low stocking density ($\leq$8 $kg{\cdot}m^{-3}$) and fish were fed high-quality aquaculture dry pellets (Amber Neptun, produced by Skretting, Norway) *ad libitum* three times per week. Within-tank temperatures in Experiment 1 varied by about 0.5°C but were more stable in Experiment 2 ($\pm$0.04°C) due to the advanced, automated control systems. Throughout the experiments, all individuals were regularly collected and anaesthetized (Finquel, 0.6 $g{\cdot}L^{-1}$), and total length and round body weight measured. In parallel, oocytes were sampled using gonad catheterization (Pipelle®, Laboratoire C.C.D). The ovarian tissue (~0.25 g) was preserved in 3.6% formaldehyde for automatic image analysis.

During Experiment 1, samples were collected every 4 weeks (6 Oct 2005, 2 Nov, 6 Dec, and 10 Jan 2006), from a total of 33 and 38 females, in the 5 and 9.6°C tanks, respectively. The fish belonging to Experiment 2 were sampled every 3–5 weeks (1 Oct 2018, 19 Nov, 18 Dec, 17 Jan 2019, 2 Feb, 18 Feb, 3 March, 18 March, and 1 April), with an average of 5 times from a total of 16, 20, 23, and 23 females, in the 3, 6, 9, and 12°C tanks, respectively. Individuals that had started spawning were no longer sampled.

Field sampling of oocytes

Oocytes were also sampled from wild-caught Atlantic cod at two locations: Austevoll (2020 and 2021) and Smøla (2019) (Fig. 1). This sampling was conducted in relation to a fish tagging effort of local Norwegian coastal cod (see also below section 'Vitellogenic temperature trajectories'). At both locations, individuals were caught using baited pots and gillnets and kept in sea cages for a maximum of three weeks prior to tagging and measurements, which took place 27–29 Jan (2020 and 2021) at Austevoll and 11–12 Feb (2019) at Smøla. The fish were anaesthetized, tagged, and measured for length and weight. For females, oocytes were sampled using gonad catheterization and preserved in 3.6% formaldehyde for image analysis. After sampling, individuals were released. In total, 40 (2020, mean total length and weight: 65.8 [62.3, 69.4] cm, 3.2 [2.7, 3.8] kg) and 19 (2021, 62.4 [57.8, 67.0] cm, 2.4 [1.9, 2.9] kg) cod were sampled for oocytes at Austevoll, and 78 at Smøla (2019, 62.4 [60.2, 64.6] cm, 2.4 [2.2, 2.6] kg). For further details, consult

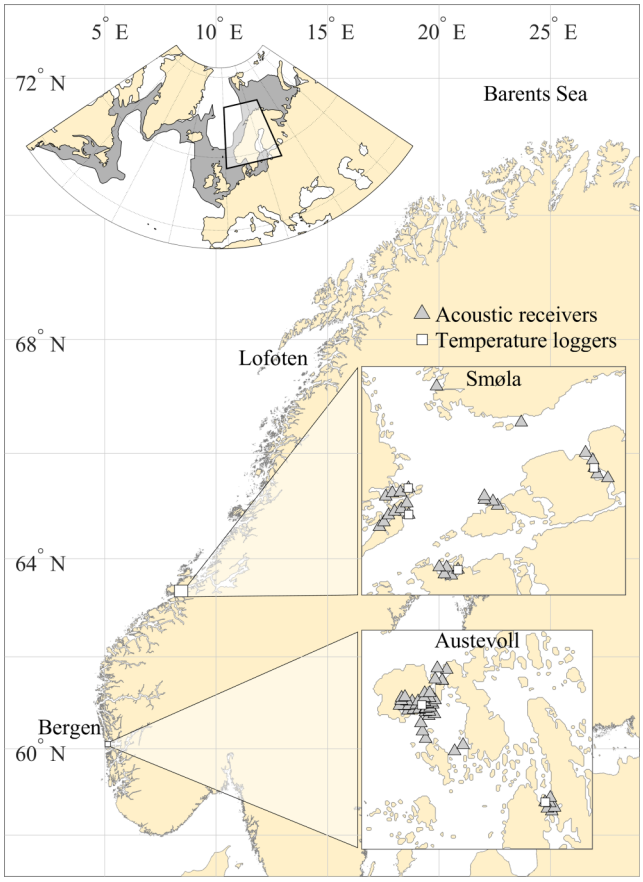

Figure 1 Field sites for wild Atlantic cod oocyte sampling and acoustic telemetry along the Norwegian coast. Oocyte samples were sampled at Smøla in 2019 (78 fish) and Austevoll in 2020 and 2021 (59 fish). In addition, acoustic telemetry networks provided near-daily vitellogenic temperature recordings (September–April) for 15 fish at Smøla (2018–2019) and 9 fish at Austevoll (2019–2021). The insert shows the whole distribution area of Atlantic cod (grey shading), and the marked frame the location of the Norwegian coast.

McQueen et al. (2022) for the Austevoll samples and Skjæraasen et al. (2021) for the Smøla samples.

Image analysis of oocyte diameter and histology

For all samples, the preserved ovarian tissue from both laboratory and field was processed automatically to measure the diameter (μm) of a minimum of 200 oocytes per individual using the autodiametric method (Thorsen and Kjesbu 2001) and the software ImageJ (v. 1.52) with the ObjectJ plugin (Schneider et al. 2012). From these measurements, the mean oocyte diameter (D_{MN}, μm) and the mean leading cohort (LC) oocyte diameter (D_{LC}, μm) for each individual were estimated. The LC was estimated as either the mean of the 10% largest vitellogenic oocytes (Experiment 1) or as the 95th percentile of all oocytes (Experiment 2). The difference between the two estimation methods is negligible. A subset of ovarian samples from Experiment 2 was also processed for histological analysis such as described in Anderson et al. (2020) to characterize the oocyte developmental stage (i.e. late vitellogenic, germinal vesicle migration I).

Statistical model of temperature-dependent oocyte development

To estimate the oocyte developmental rate as a function of temperature and leading cohort oocyte diameter (D_{LC}), we constructed a statistical model for the experimental data. We included data at the tank level until the first female started spawning, and any measurements of $D_{LC} > 800$ μm were excluded, as we expect such large oocytes to develop differently due to final oocyte maturation (Craik and Harvey 1987, Kjesbu 1989). After removal of the largest oocytes, a total of 687 diameter measurements remained. We then calculated the oocyte growth rate (R, μm·day^{-1}) as the diameter difference divided by time between two successive measurements. The few cases of negative rates ($N = 53$) were removed, leaving a total of 526 growth estimates for further analysis. A first analysis of the data using a generalized additive model (GAM, Wood 2017) indicated two developmental 'phases', with an accelerating phase up to a D_{LC} of about 650 μm, followed by a more variable phase for larger oocytes. For the last phase ($D_{LC} >$ 650 μm), neither temperature nor oocyte size could explain the variation in oocyte growth rates, but from an earlier study, we know that spawning is initiated around 2–3 weeks, depending on temperature, after the leading cohort oocytes reaches 650 μm in diameter (Kjesbu 1994). Since one of the aims of our study was to develop a functional relationship between oocyte developmental rates and these covariates, we focused on the relatively linear phase ($D_{LC} < 650$ μm), and started with the following model

$$R_i \sim D_{LC_i} \times T_i + D_{LC_i} \times Length_i + T_i \times Length_i + Day_i + Exp_i + Ind_i \quad (1)$$

where is R_i the oocyte growth rate (μm·day^{-1}) for observation i, $D_{LC}i$ is the associated mean leading cohort oocyte diameter (μm), T_i is the temperature (°C), $Length_i$ and Day_i are the mean fish (total) length (cm), and the mean day-of-year associated with R_i, respectively, and Exp_i is a factor describing the experiment (1 or 2). Finally, a random effect of Ind_i was included to account for repeated measurements on individual fish. We performed a model selection by the function 'dredge()' in the MuMIn package (Bartoń 2024). All variables contained in the models with ΔAIC < 2 compared to the top model were retained, and this model was refitted and used further. Also, a non-parametric bootstrap based on the selected model was performed to estimate the regression uncertainty and to account for the individual variability in gonad development—a routine that included resampling individuals within each experiment 1000 times, hence constructing 1000 equally likely model versions.

Finally, we also fitted a series of degree-day models to the experimental data and compared the output to the best statistical model. We first calculated the observed oocyte development trajectories from 450 to 650 μm for the 153 individual fish held at 6 different temperatures and then noted the different individual development times (days from 450 to 650 μm). From these calculations, we constructed 6 different degree-day models, configured to the mean development time at each temperature.

Vitellogenic temperature trajectories

To predict oocyte development (R, μm·day^{-1}) in the field based on the statistical model derived from the temperature-controlled experiments, we needed information on the ambient vitellogenic temperature, i.e. the daily temperature that an individual experienced during the period between the start of vitellogenesis [here defined as $D_{LC} = 250$ μm *sensu* Kjesbu et al. (2010)] in the autumn and the end of vitellogenesis shortly before oocyte hydration and spawning (here defined as $D_{LC} = 650$ μm) the following spring (Kjesbu et al. 2010).

We utilized depth and temperature information from 560 mature cod with acoustic tags from Innovasea (formerly Vemco) surgically placed in the abdominal cavity under sedation (see also the above section Field sampling of oocytes). Of these, there were 217 (Austevoll) and 194 (Smøla) V13P tags transmitting ambient depth (P), and 149 (Smøla) V13TP tags transmitting both ambient temperature (T) and depth (P). All tags transmitted data on average every 250 seconds within an array of 27 and 51 acoustic receivers at Austevoll (2019–2021) and Smøla (2018–2019), respectively (triangles in Fig. 1). In addition, temperature loggers at fixed depths (1, 5, 10, 15, 20, 25, 30, 40, 50, 60, 70, 80 m) stored temperature with bi-hourly resolution at both locations: 2 at Austevoll and 4 at Smøla (squares in Fig. 1). Ambient fish temperatures for individuals with V13P tags were estimated by looking up each transmitted depth (P) at the nearest temperature logger (T_{INT}, linearly interpolated to tag depth) such that the estimated ambient temperature $T_E \sim T_{INT}(P)$. The accuracy was examined by comparing the tag-transmitted temperature T and nearest-logger-estimated temperatures T_E from the 149 V13TP tags in Smøla that transmitted both P and T using a major axis regression linear model (Sokal and Rohlf 2012). From the 560 individual temperature trajectories (T and T_E), we located a total of 24 individuals (60.2 [56.8, 63.6] cm, 2.4 [2.0, 2.9] kg) with near-continuous (max permitted gap between recordings was 14 days) temperature recordings between September and March and thus represent complete coverage of individual vitellogenic temperature.

Back-calculating the start day of oocyte development in the field

Starting with the oocyte diameters observed in the field (D_{LC}), we used daily vitellogenic temperature (observed or modelled) as input to the statistical model of oocyte growth rates to back-calculate the respective oocytes to a diameter of 250 μm. Back-calculation was constrained to individuals with $D_{LC} \leq 650$ μm, which is the set upper boundary of the model (see above).

Depending on the information available for each individual fish, we applied two different approaches. For sampled individuals with information on both oocyte diameter and preceding vitellogenic temperature (from tags), we back-calculated oocyte development for each individual separately. For sampled individuals with only oocyte diameter, we back-calculated the oocyte development based on the average vitellogenic temperatures (from tags) from other individuals being tracked within the same location during the pre-spawning season. These calculations were also used to estimate the probability distribution of 'start-dates' for vitellogenesis, i.e. the date when $D_{LC} = 250$ μm. We did this by finding the best-fitting cumulative probability density function (mean

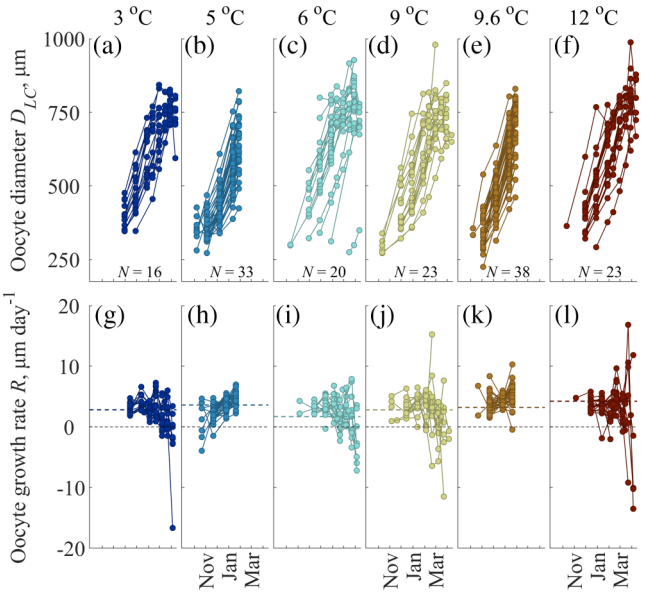

Figure 2 Atlantic cod oocyte diameter and growth rate at different temperature treatments. The upper (a–f) and lower (g–l) panels show the development of the mean diameter of the leading cohort of oocytes (D_{LC}, μm) and the corresponding growth (R, μm day^{-1}), respectively, of 153 Atlantic cod kept at 3, 5, 6, 9, 9.6, and 12°C between October and April. *N* indicates the number of fish in each temperature treatment, while the solid lines denote the temporal trajectory of each individual. Individuals were sampled on average 4–5 times during each temperature treatment (circles in upper panels). In panels g–l, coloured dashed horizontal lines indicate the mean oocyte growth rate, while dashed black lines denote zero growth.

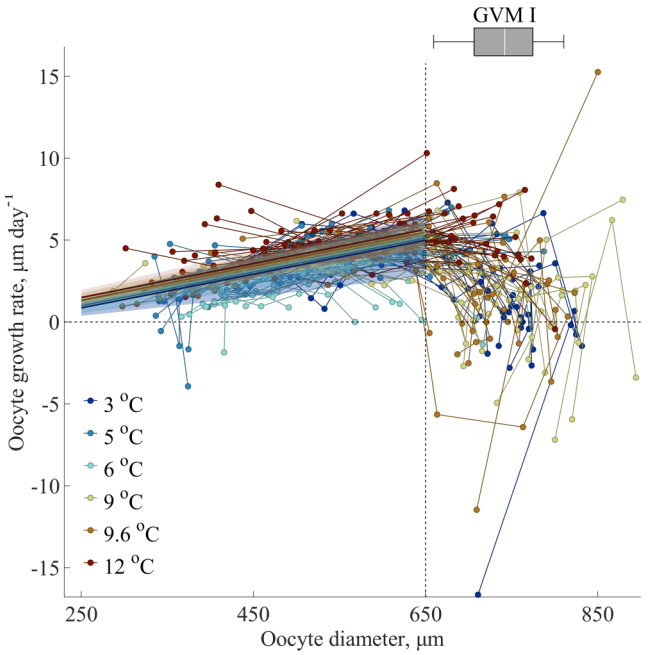

Figure 3 Observed and modelled relationships between oocyte diameter and growth rate for Atlantic cod at different temperatures. Circles and thin connecting lines denote the observed temporal trajectory of a single individual's mean leading cohort oocyte diameter (D_{LC}, μm) and the corresponding growth rate (*R*, μm day^{-1}), as shown in the upper and lower panels of Fig. 2, respectively. Colours indicate water temperature of each treatment (*T*,°C). Thick straight lines and shaded area show the statistical model (Eq. 2) mean and the 95% CI, respectively, for each temperature treatment.

$R = -1.96 + 0.01.D_{LC} + 0.07.T$

The model was constrained to observed $D_{LC} \leq 650$ μm, shown with vertical dashed line. The box-and-whiskers plot denotes the median (white line), the 25th and 75th percentiles (box), and the 10th and 90th percentiles (whiskers) of oocyte diameters in the germinal vesicle migration 1 stage (GVM I) from Experiment 2.

and standard deviation) to the back-calculated dates when $D_{LC} = 250$ μm.

Results

Experimental data and model for oocyte development

Across all temperature treatments (3, 5, 6, 9, 9.6, and 12°C), a total of 684 ovarian (oocyte) samples were drawn from 153 individuals. In general, the leading cohort oocyte diameter (D_{LC}) increased over time (Fig. 2a–f). The corresponding series of oocyte growth rates (*R*, $N = 342$), calculated at the midpoint between each D_{LC} measurement, was thereafter plotted (Fig. 2g–l). Overall, there was no clear pattern between average growth rates across the entire experimental period and temperature treatment, although it increased gradually from 6 to 12°C. However, when data was pooled across all temperature treatments, the larger sample size made it clear that oocyte growth rates first accelerated as oocyte diameter increased (Fig. 3), and then became highly variable and frequently negative towards the end of the experimental period. The preliminary GAM analyses and visual inspection of Fig. 3 indicated that for oocyte diameters >650 μm, there was an apparent deceleration of growth. From the histology, we noted that oocytes started entering the germinal vesicle migration 1 stage (GVM I) at around this size (Supplementary Table S1 and Fig. 3). Beyond 650 μm variability also increased, and growth rate development could no longer be explained by the available covariates. Hence, the statistical model was constrained to oocyte diameters ≤650 μm. The final best-fit model (Supplementary Table S2, based on Eq. 1) suggested that oocyte growth rate (*R*, μm·day^{-1}) was linearly related to the mean leading cohort oocyte diameter (D_{LC}, μm) and temperature (*T*,°C), such that

$$R = \beta + \alpha \cdot D_{LC} + \gamma \cdot T, \quad (2)$$

where $\beta = -1.96$ [−2.9, −1.0], $\alpha = 0.01$ [0.009, 0.012], and $\gamma = 0.07$ [0.025, 0.12]. Here, bracketed values denote the 95% CI of each parameter following from the non-parametric bootstrap. Note that we added half the experimental factor to the intercept to get a mean model. The model predictions for the different temperature treatments were contrasted; there was a clear effect of temperature and oocyte diameter, but confidence intervals overlap among temperature treatments (Fig. 3).

Assuming an initial oocyte diameter of 250 μm at the cortical alveoli stage, the model focuses on the subsequent vitellogenic period and was used to predict the number of days it would take the oocyte to reach 650 μm at different temperatures (Fig. 4). At water temperatures of 2°C, oocyte development was predicted to take on average 178 [147, 246] days. In comparison, a temperature

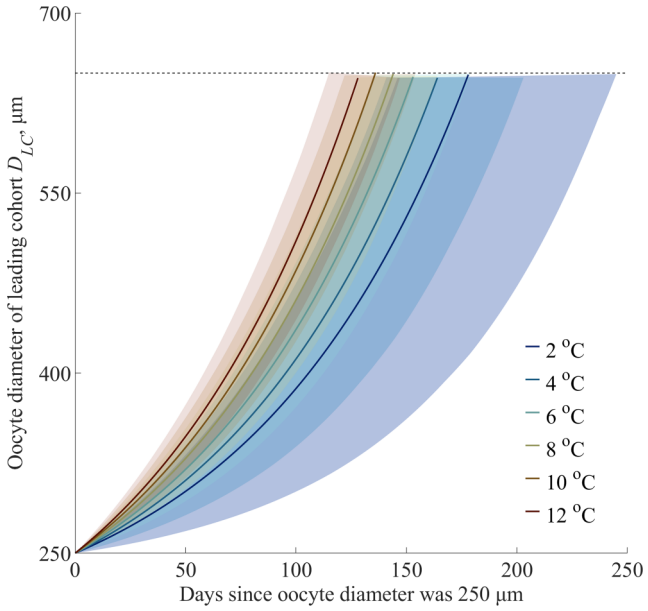

Figure 4 Statistical prediction of oocyte development time for Atlantic cod at different temperatures. Based on the statistical model (Eq. 2 and Fig. 3), the average time (days) for an oocyte to grow from 250 to 650 μm is given for 6 different temperatures (coloured lines). Shaded areas denote the corresponding 95% CI of the model mean. Note that an increase in water temperature from 2 to 4°C speeds up the mean oocyte development time (250–650 μm) by 14 days (7 days faster per °C), whereas an increase from 10 to 12°C speeds up the development time by 8 days only (4 days faster per °C).

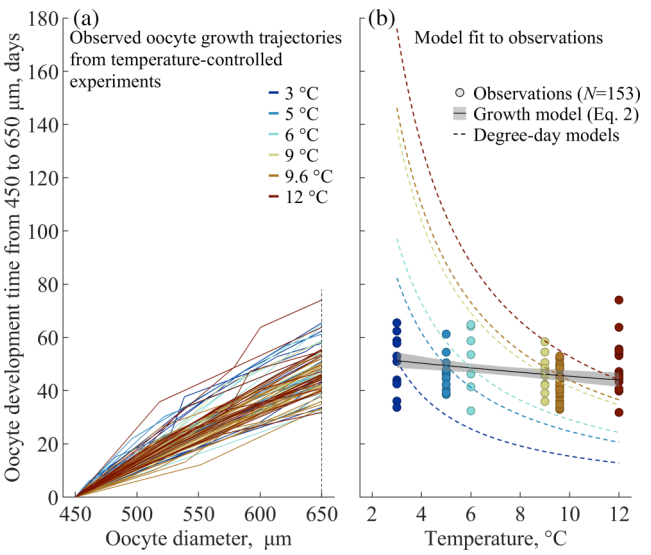

Figure 5 Comparing the oocyte growth model and degree-day models with observations. Panel a shows the observed oocyte development trajectories from 450 to 650 μm (dashed vertical line) for 153 individual fish held at 6 different temperatures. In panel b, the circles show the total development time (450–650 μm) at each temperature (colours and x-axis). The solid line and shading are the mean and 95% CI of the oocyte development time as predicted by the oocyte growth model (Eq. 2). Dashed lines show 6 different degree-day models, configured to the mean development times at each temperature.

of 4°C reduced average development time to 164 [142, 204] days. The effect of increasing temperature on oocyte development time diminished as temperature increased further. An increase in water temperature from 2 to 3°C shortened the mean oocyte development time by ca 7 days, while an increase from 10 to 11°C only by around 4 days.

When compared to the 6 different degree-day models (Fig. 5), it is evident that oocyte development at different temperatures (Fig. 5a) is difficult to capture using a degree-day metric (Fig. 5b). Overall, the degree-day models suggest a markedly higher sensitivity of development time to temperature than indicated by the experimental data.

Field data and back-calculation of oocyte development

The assumption that ambient temperature for fish with only depth sensors (V13P-tags) could be approximated by looking up the temperature at the relevant depth at the nearest temperature logger (T_E) was checked with major axis regression: $T_E \sim \beta + \alpha.T$, where T_E and T are the estimated and ambient temperature, respectively, for the 149 fish at Smøla (September–April) that also transmitted temperature ($N = 778\,306$). The regression yielded $\beta = 0.818$ [0.815, 0.822], $\alpha = 0.9374$ [0.9369, 0.9379], with $R^2 = 0.94$, suggesting a close relationship (Supplementary Fig. S1) between the two variables so they could be used interchangeably in the further analysis.

In Fig. 6 we show daily vitellogenic temperature from acoustic tags (Fig. 6a) and the corresponding calculated oocyte development (Fig. 6b) for two single individuals that were first captured and tagged then tracked from early September until re-capture close to spawning at Smøla (11–12 Feb 2019) and Austevoll (28 Jan 2021), when oocyte diameter was also subsequently measured.

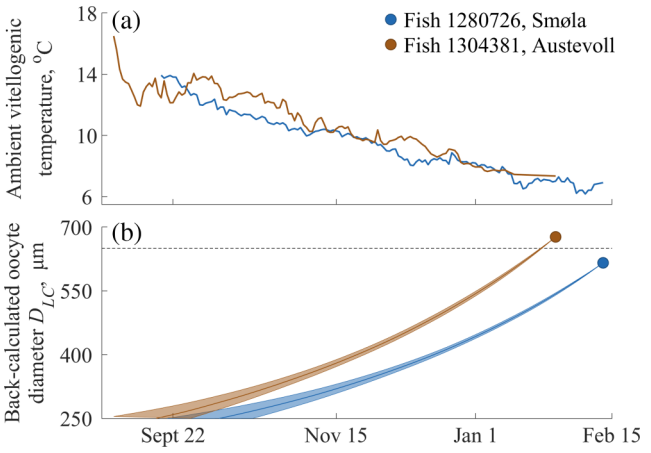

Figure 6 Detailed field tracking of oocyte development and experienced temperature conditions of two individual Atlantic cod. Panel a denotes the observed ambient vitellogenic temperature trajectory (from acoustic tags) in the period September-February for the female off Smøla in 2019 and at the one off Austevoll in 2020 (Fig. 1). In panel b, circles show the mean leading cohort oocyte diameter (D_{LC}, μm) at re-capture of the same two individuals. Lines and shading are the corresponding backwards statistical model (Eq. 2) predicted mean oocyte diameter, and the 95% CI of the model mean, respectively. Horizontal dashed line marks the 650 μm oocyte threshold.

Back-calculated developmental trajectories of oocyte growth using experienced vitellogenic temperature (Fig. 6a) as input to the oocyte growth model (Eq. 2) suggested that the fish at Smøla started vitellogenesis around 30 September, ca 10 days later than the fish at Austevoll (Fig. 6b).

For the same two locations, a total of 24 continuous individual vitellogenic temperature trajectories (from acoustic tags) were available for the years 2018–2021, as well as oocyte diameters of 137 individuals sampled in parallel. At Smøla, average daily vitellogenic temperature was calculated as the daily mean of 15 individuals (2018–2019, Fig. 7a) and used to back-calculate oocyte development of 44 individuals sampled on 11–12 Feb in 2019 (Fig. 7d). The same was done for Austevoll, where daily mean vitellogenic temperatures were estimated based on the mean of 5 (2019–2020, Fig. 7b) and 4 (2020–2021, Fig. 7c) individuals, and used to back-calculate oocyte development for 25 and 13 different individuals sampled for oocytes on 28–29 Jan in 2020 (Fig. 7e) and 27–28 Jan in 2021 (Fig. 7f), respectively.

An additional 55 individuals were sampled (Fig. 7d–f, black dots) but had oocyte diameters outside the model boundaries (D_{LC}>650 μm), and oocyte development was therefore not back-calculated. However, these individuals were included to estimate the median and percentiles of all sampled individuals (Fig. 7d–f). The lower median oocyte diameter at Austevoll (591 μm) compared to Smøla (625 μm) aligns well with the model predictions given the differences in sampling dates and temperature (Supplementary Fig. S2).

For the individuals with back-calculated oocyte development, we also established the probability distribution of the date at which D_{LC}=250 μm, here referred to as start date for vitellogenesis. The estimation was done by fitting a cumulative probability function to the individual start dates (Fig. 7g–i). The predicted start-date probabilities of the best-fitting functions (Pr_E) were then compared to the observed data (Pr) in each location using a simple linear regression, $Pr_E \sim \beta + \alpha . Pr$. For all regressions, model parameters were within the following 95% CI: $\beta \sim 0$ [−0.09, 0.1], $\alpha \sim 1$ [0.9, 1.1], and $R^2 > 0.96$. Mean start dates were predicted to fall between 29 September and 3 October, with a standard deviation between 24 and 32 days depending on year and location (Fig. 7j–l).

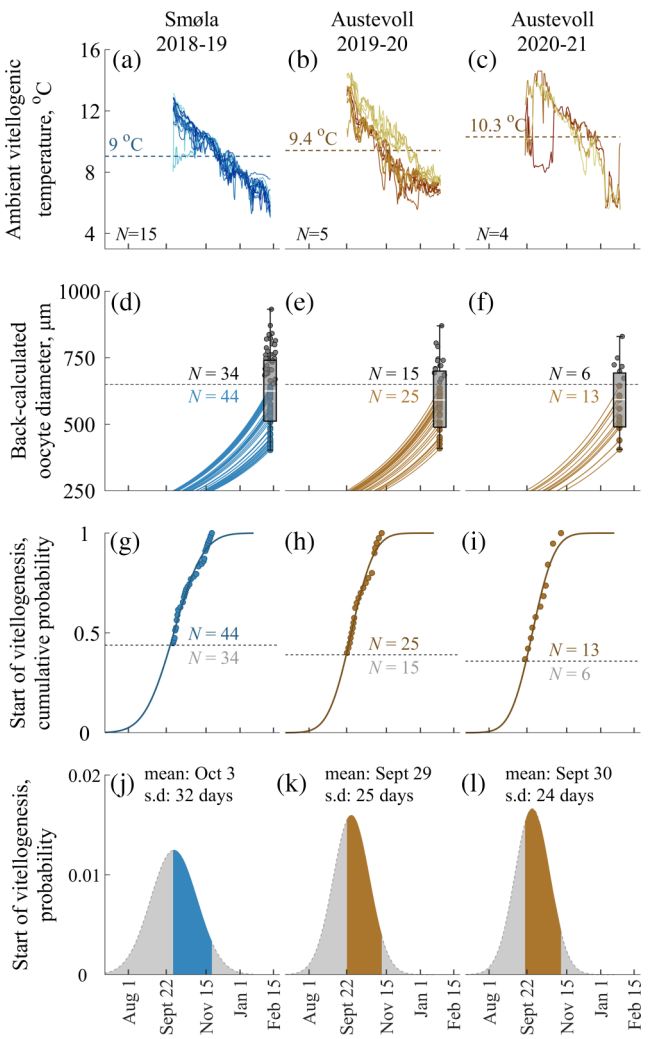

Figure 7 Field observations and model back-calculation of oocyte development and vitellogenic start day of Atlantic cod. Panels a–c show the ambient vitellogenic temperatures (from acoustic tags) of 24 individuals at Smøla and Austevoll (Fig. 1) in three different year spans (*N:* number of individuals). The dashed lines and numbers indicate the mean vitellogenic temperatures. Panels d–f show the mean leading cohort oocyte diameter (D_{LC}, μm) of 137 cod captured in parallel in the same two areas and years. The box-and-whiskers plots (d–f) represent the median (white line), the 25th and 75th percentiles (box), and the 10th and 90th percentiles (whiskers) for all fish captured at Smøla in 2019, and at Austevoll in 2020 and 2021. Dashed horizontal lines indicate 650 μm, and oocyte diameters above or below this threshold are marked with grey or coloured dots (and *N*), respectively. For the latter, the statistical model (Eq. 2) is used to back-calculate mean oocyte diameter to the start of vitellogenesis at 250 μm (solid lines) based on the average temperature trajectories of the fish shown in panels a–c. Panels g–i show the cumulative probability for the vitellogenic start day of the same fish. Solid lines represent the best-fit cumulative distribution, while horizontal dashed lines show the 650 μm cutoff. Panels j–l show the reciprocal probability density functions, where areas outside or within the range of back-calculated start days are shaded in grey or colour, respectively. Mean and standard deviation (s.d.) of estimated vitellogenic start day for each location and year are denoted.

Discussion

We have presented original insights into the oocyte growth dynamics in Atlantic cod by synthesizing new and past data. We report a statistically significant relationship between experimental temperature and the growth rate of vitellogenic oocytes, and validate its performance against field observations. At the individual level, the relationship between temperature and oocyte growth rate held until 650 µm diameter, suggesting that beyond that size other processes than temperature-dependent growth determined the speed of oocyte maturation. Further, we demonstrated that at the population level, the between-individual variation in oocyte growth rates is comparable in magnitude to the effect of temperature itself. Together, our results suggest that there is flexibility and variation at both the individual and population levels that influence to what degree temperature can modulate reproductive timing—likely an important feature for maximizing spawning success.

Temperature-dependent model of oocyte development

From the temperature-controlled experiments, we found that oocyte growth rates increased with increasing temperatures. This outcome aligns with a range of earlier studies from both marine and freshwater species that have shown faster gonadal development in warmer water, including in Atlantic cod (Yoneda and Wright 2005, Kjesbu et al. 2010), Caspian roach *Rutilus rutilus caspicus* (Akhoundian et al. 2020), walleye pollock (Tanaka et al. 2019), European eel *Anguilla anguilla* (Kucharczyk et al. 2016), and pikeperch *Sander lucioperca* (Ljubobratovic et al. 2024). However, depending on the amplitude and timing during the reproductive cycle, a warmer water temperature can also slow down or arrest gonad development (Wright et al. 2017, Anderson et al. 2020).

In our data, oocyte growth rates, measured in diameter increment per time, accelerated with oocyte size, such that oocyte diameter increased more rapidly towards the end of vitellogenesis, closer to spawning. While an earlier study on Atlantic cod showed a similar accelerating pattern (Kjesbu 1994), it contrasts more recent laboratory experiments (Experiment 1, embedded in this study) using tank-averages, and where growth rates were reported to be constant over time (Kjesbu et al. 2010). When we reanalysed these data with focus on individual-level effects, accelerating growth rates were detected for the data from Experiment 1. For Atlantic herring *Clupea harengus*, contrasting patterns of oocyte growth have also been observed, with experimental data suggesting accelerating growth (Ma et al. 1998) and field data indicating either linear (Kurita et al. 2003) or accelerating growth (Óskarsson et al. 2002). Further, the European pilchard *Sardina pilchardus* has accelerating oocyte growth (Ganias et al. 2011), while no clear pattern is apparent for Pacific herring *Clupea pallasii* (Hay et al. 1988). An important finding is the considerable variation in oocyte growth rates, both within and among temperature treatments. This deduction was indeed the case in Kjesbu et al. (2010), briefly explored in Opdal et al. (2024b) but not formalized or incorporated into predictive models for oocyte growth or spawning time. Also, the large fluctuation and variation in oocyte growth rates when $D_{LC}>650$ μm suggest that the oocytes are influenced by a different type of endocrine process associated with the germinal vesicle migration (e.g. Cerdà et al. 2007) or related to the surges in luteinizing hormone (LH) and maturation-inducing hormone (MIH) during the final oocyte maturation stage (FOM) (Alix et al. 2020)). These processes likely have different temperature sensitivity. As such, we should expect even larger variability in the onset of first spawning than captured by the model uncertainty in oocyte growth up to 650 μm. Large variability also exists in oocyte development for other species, such as for Atlantic herring (Ma et al. 1998), European pilchard (Ganias et al. 2011), and Pacific herring (Hay et al. 1988). However, individual variation is often not shown, and if shown, it is removed through averaging when constructing oocyte development models. While averaging across individuals is a common way to reduce random noise and measurement error, it can also mask the potential, and largely unquantified, role of behavioural and physiological plasticity and portfolio effects at the population level.

Another source of variation is related to the oocyte measurements themselves. Considering that the ovarian catheterization procedure for each individual cannot sample the same oocyte twice, and possibly samples partly different regions of the gonad each time, we expect some variation in the leading cohort oocyte size (LC). This variation is especially evident at the later stages ($D_{LC}>650$ μm), as can be inferred from the frequent occurrence of negative growth rates. Although several studies have demonstrated that the cod ovary is fully homogeneous and that different sampling locations in the ovary should not influence oocyte diameter estimate (Witthames et al. 2009), the size distribution of the vitellogenic oocytes widens over development time (Kjesbu et al. 1991, Anderson et al. 2020). Hence, when the vitellogenic oocyte diameters are small, the overall size distribution of the unimodal curve is narrow and sampling variation small. However, as oocytes approach hydration and spawning, the size distribution is broader, increasing the risk of sampling bias towards either side of this mode, and particularly in the tail of the largest oocytes where the LC is quantified. To compensate, larger or repeated samples should be drawn from more advanced stages of gonadal development.

Model back-calculation and vitellogenic start dates from field data

The back-calculated oocyte developments at Austevoll and Smøla predicted that (endogenous) vitellogenesis (assumed to begin from $D_{LC}=250$ μm) on average started between 29 September and 3 October, with a probability distribution covering several months between August and December. Near the mean of the probability distribution, we also found the start dates of the two recaptured individuals that had carried acoustic tags that transmitted ambient temperature and for which oocyte diameter was measured at recapture (Fig. 6). For the remaining wild-caught individuals, overall mean start date across locations and years (2019–2021) was 1 October $\pm$ 7 days (95% CI). This date is remarkably close to autumn equinox (22–23 September), as first proposed as the general start date for cod vitellogenesis by Woodhead and Woodhead (1966) and later supported by findings of Kjesbu et al. (2010). However, the wide distribution implies that ca 95% (mean $\pm$ 2 s.d.) of individuals start vitellogenesis within a 4-month period between 1 August and 2 December, while only around 20% (mean $\pm$ 0.5 s.d.) have start dates within $\pm$ 1 week of the mean. Similar variation in vitellogenic start dates has been quantified in experimental studies, and reported to be $\pm$ 1 month for Atlantic cod (Kjesbu et al. 2010) and several months in Atlantic herring (Ma et al. 1998).

These results strongly suggest considerable variation not only in the individual rate of oocyte development (captured by the model uncertainty), but also in the start date, which at the population level may span several months. Against this backdrop, it seems an oversimplification to assume onset of vitellogenesis at a fixed date such as autumn equinox, even though the date does provide an intriguing, globally synchronized, daylight cue (Woodhead and Woodhead 1966). Also, such a cue is unable to explain the occurrence of vitellogenic start dates prior to the cue itself, as seen here and in other studies (Kjesbu et al. 2010). For autumn-spawning Atlantic herring, it is shown that multiple light cues are in play (winter solstice and spring equinox) (Santos et al. 2006), suggesting that summer solstice might be relevant for the spring-spawning cod. Although body length has been found to influence oocyte growth at certain temperatures (Kjesbu et al. 2010), we did not observed such an effect—neither in the tank experiments nor

in the field. Variation could, however, arise from individual differences in photic sensitivity (*zeitgeber*) or the timing of the circadian clock (Ekstrom and Meissl 1997, Krylov et al. 2021), heritable traits related to spawning time (Otterå et al. 2006), or in the utilization of some additional, but unknown environmental cues. Such variation in start date may outweigh the statistical effects of temperature, with the consequence that the model's ability to predict oocyte development will decrease although the flexibility of cod to time spawning successfully may improve. However, if assuming that vitellogenesis indeed begins around autumn equinox, the current model with accelerating oocyte growth performs well in predicting these field observations and perform better compared to an earlier derived linear growth model, which tends to predict start of spawning somewhat later than observed (Kjesbu et al. 2010).

Also, it should be mentioned that the experimental tanks were supplied by water from inlets located well below the upper mixed layer, where at least the water at the station at Matre passed through several cleaning filters. A lack of planktonic organisms creates a different biotic environment in the laboratory compared to the field, which could influence developmental rates closer to spawning (Opdal et al. 2024a, Opdal et al. 2024b), but probably less so earlier in the vitellogenic phase. Moreover, the apparent cessation of oocyte growth at larger oocyte sizes might suggest some sort of arrested development mechanisms while awaiting additional environmental cues like early bloom onset or water column stratification (Opdal et al. 2024b).

A statistical limitation of our data is that vitellogenic temperature trajectories were drawn from only 24 individuals. While these fish on inspection represent well the 171 tagged fish (∼31%) consistently or occasionally present in the area during more than half the vitellogenic period (August–January), it is difficult to know what temperatures the other 389 fish outside the telemetry arrays were experiencing. They could be nearby in similar coastal waters, or offshore in quite different Atlantic water masses.

We also note that experiments and field data in our study concern the Norwegian coastal cod population, a sub-population inhabiting a small corner of Atlantic cod's vast distribution area. To what degree the findings are representative for the total range of the species' genotypic and phenotypic plasticity is uncertain. However, we believe that our model, even though it is based on a small geographical subset, performs better and is more rigorously tested than earlier models for Atlantic cod. Moreover, the phenotypic variability described for the Norwegian coastal cod is likely a conservative estimate, and that if measured for the Atlantic cod population as a whole, we should expect it to be much larger. Still, other regional subsets of the Atlantic cod may have lower phenotypic plasticity.

Conclusion

Compared to previously published models for Atlantic cod (Kjesbu et al. 2010) and fish in general (Asch et al. 2019), we find moderate changes in oocyte development times with temperature. This result aligns with earlier findings that temperature is a rather poor predictor of interannual variation in Atlantic cod spawning time (Opdal et al. 2024a, Opdal et al. 2024b). Other studies, e.g. McQueen and Marshall (2017), have found that earlier spawning of North Sea cod correlated with increasing surface temperatures. However, our findings do not negate that temperature influences oocyte development of fish, as is demonstrated here and in other studies (Ware and Tanasichuk 1989, Kjesbu et al. 2010, Pankhurst and Munday 2011, Skjærven et al. 2024), but do suggest that additional factors also play an important role in determining spawning time. Our study focused on oocytes and cannot conclude on how temperature may affect later processes that influence timing of spawning. The high individual variation may well reflect plasticity, which likely constitutes an important part of the uncertainty of oocyte growth rate models. Evolutionarily, this makes sense: considering how decoupled e.g. the phytoplankton spring bloom is from the temperature alone (Sverdrup 1953, Behrenfeld 2010), we should expect strong selection for the ability to at least partly decouple spawning time from temperature. While several studies report correlations between temperature and fish spawning time (Pankhurst and Munday 2011, Poloczanska et al. 2016, McQueen and Marshall 2017, Rogers and Dougherty 2019), a fuller analysis of residual variation has to our knowledge not been done. Where timing of spawning relatively to other ecological processes is studies, there are rarely signs of decoupling from lower trophic levels (Samplonius et al. 2021). Our findings might add nuance to the conclusion of the recent IPCC (AR6 WGII) report that 'temperature-linked phenology of fish reproduction (…) will likely cause phenological mismatches resulting in increased risk of starvation for fish larvae (medium to high confidence)' (Cooley et al. 2022). Specifically, our findings suggest that the temperature effect is smaller than previously documented and that the large individual variation that might reflect phenotypic plasticity should caution against the use of models that apply mean thermal effects to predict spawning timing and performance for groups or populations. Hence, other detailed case studies such as this one but on other species are clearly needed.

Acknowledgements

We thank two anonymous reviewers for their constructive comments and helpful suggestions, which greatly improved the clarity and quality of this manuscript.

Author contributions

Anders Frugård Opdal (Conceptualization [equal], Data curation [equal], Formal Analysis [equal], Funding acquisition [equal], Methodology [equal], Project administration [equal], Visualization [equal], Writing – original draft [equal], Writing – review & editing [equal]), Maud Alix (Data curation [equal], Formal Analysis [equal], Investigation [supporting], Methodology [supporting], Writing – original draft [supporting], Writing – review & editing [supporting]), Olav Sigurd Kjesbu (Data curation [equal], Formal Analysis [equal], Funding acquisition [equal], Investigation [supporting], Methodology [supporting], Writing – original draft [supporting], Writing – review & editing [supporting]), Christian Jørgensen (Conceptualization [equal], Formal Analysis [supporting], Investigation [supporting], Writing – original draft [equal], Writing – review & editing [equal]), Øystein Langangen (Formal Analysis [equal], Investigation [equal], Methodology [equal], Writing – original draft [supporting], Writing – review & editing [supporting]), Daniel Nyqvist (Data curation [supporting], Formal Analysis [supporting], Investigation [supporting], Writing – original draft [supporting], Writing – review & editing [supporting]), Ørjan Karlsen

(Data curation [supporting], Formal Analysis [supporting], Funding acquisition [equal], Investigation [supporting], Methodology [supporting], Writing – original draft [supporting], Writing – review & editing [supporting]), Kate McQueen (Data curation [supporting], Investigation [supporting], Methodology [supporting], Writing – original draft [supporting], Writing – review & editing [supporting]), Esben Moland Olsen (Data curation [supporting], Funding acquisition [equal], Methodology [equal], Writing – original draft [supporting], Writing – review & editing [supporting]), Anders Thorsen (Data curation [supporting], Formal Analysis [supporting], Methodology [equal], Writing – original draft [supporting], Writing – review & editing [supporting]), Jon Egil Skjæraasen (Conceptualization [equal], Data curation [equal], Formal Analysis [equal], Funding acquisition [equal], Investigation [equal], Methodology [equal], Writing – original draft [supporting], Writing – review & editing [supporting])

Supplementary data

Supplementary data is available at *ICES Journal of Marine Science* online.

Conflicts of interest

None declared.

Funding

The work was supported by Thermos 354612 (A.F.O., J.E.S., and C.J.), ScaleClim 268336 (C.J., A.F.O., M.A., O.S.K., and J.E.S.), and SpawnSeis 280367 (J.E.S., E.M.O., Ø.K., K.M.Q., D.N., and Ø.L.), all financed by the Research Council of Norway. In addition, J.E.S., E.M.O., and Ø.K. also received funding from ICOD 901230 financed by FHF—Norwegian Seafood Research Fund.

Data availability

The data underlying this article are available in Dryad at https://doi.org/10.5061/dryad.08kprr5cs

References

Akhoundian M, Salamat N, Savari A *et al.* Influence of photoperiod and temperature manipulation on gonadal development and spawning in Caspian roach (*Rutilus rutilus caspicus*): implications for artificial propagation. *Aquaculture Research* 2020;**51**:1623–42. https://doi.org/10.1111/are.14509

Alix Maud, Kjesbu Olav S., Anderson Kelli C. From gametogenesis to spawning: How climate-driven warming affects teleost reproductive biology. *Journal of Fish Biology*, 2020;**97**:607–632. https://doi.org/10.1111/jfb.14439

Anderson KC, Alix M, Charitonidou K *et al.* Development of a new 'ultrametric' method for assessing spawning progression in female teleost serial spawners. *Sci Rep* 2020;**10**:9677. https://doi.org/10.1038/s41598-020-66601-w

Asch RG, Stock CA, Sarmiento JL. Climate change impacts on mismatches between phytoplankton blooms and fish spawning phenology. *Glob Chang Biol* 2019;**25**:2544–59. https://doi.org/10.1111/gcb.14650

Bartoń K. MuMIn: multi-model inference. R package version 1.48.4. 2024. https://CRAN.R-project.org/package=MuMIn (01 April 2025, date last accessed).

Behrenfeld MJ. Abandoning Sverdrup's critical depth hypothesis on phytoplankton blooms. *Ecology* 2010;**91**:977–89. https://doi.org/10.1890/09-1207.1

Cerdà J, Fabra M, Raldúa D. Physiological and molecular basis of fish oocyte hydration. In: Babin PJ, Cerdà J, Lubzens E. (eds), *The fish oocyte. From basic studies to biotechnological applications*. Dordrecht, The Netherlands: Springer, 2007.

Cooley S, Schoeman D, Bopp L *et al.* Oceans and coastal ecosystems and their services. In: Pörtner H-O, Roberts DC, Tignor M. et al. (eds), *Climate Change 2022: Impacts, Adaptation and Vulnerability. Contribution of Working Group II to the Sixth Assessment Report of the Intergovernmental Panel on Climate Change*. Cambridge and New York, NY: Cambridge University Press, 2022.

Craik JCA, Harvey SM. The causes of buoyancy in eggs of marine teleosts. *J Mar Biol Assoc U K* 1987;**67**:169–82. https://doi.org/10.1017/S0025315400026436

Cushing DH. Dependence of recruitment on parent stock. *J Fish Res Board Can* 1973;**30**:1965–76. https://doi.org/10.1139/f73-320

Cushing DH. Plankton production and year-class strength in fish populations—an update of the match mismatch hypothesis. *Adv Mar Biol* 1990;**26**:249–93.

Cushing DH. Regularity of spawning season of some fishes. *J Cons* 1969;**33**:81–92. https://doi.org/10.1093/icesjms/33.1.81

Ekstrom P, Meissl H. The pineal organ of teleost fishes. *Rev Fish Biol Fish* 1997;**7**:199–284. https://doi.org/10.1023/A:1018483627058

Fincham JI, Rijnsdorp AD, Engelhard GH. Shifts in the timing of spawning in sole linked to warming sea temperatures. *J Sea Res* 2013;**75**:69–76. https://doi.org/10.1016/j.seares.2012.07.004

Ganias K, Nunes C, Vavalidis T *et al.* Estimating oocyte growth rate and its potential relationship to spawning frequency in teleosts with indeterminate fecundity. *Mar Coast Fish* 2011;**3**:119–26. https://doi.org/10.1080/19425120.2011.555729

Hay DE, Brett JR, Bilinski E *et al.* Experimental impoundments of prespawning pacific herring (*Clupea harengus pallasi*)—effects of feeding and density on maturation, growth, and proximate analysis. *Can J Fish Aquat Sci* 1988;**45**:388–98. https://doi.org/10.1139/f88-047

Hjort J. Fluctuations in the great fisheries of northern Europe viewed in the light of biological research. *Rapports et Procès-verbaux des Réunions, Conseil International pour l'Exploration de la Mer*. 1914;**20**:1–228.

Hutchings JA, Myers RA. Timing of cod reproduction—interannual variability and the influence of temperature. *Mar Ecol Prog Ser* 1994;**108**:21–31. https://doi.org/10.3354/meps108021

Kjesbu OS, Klungsøyr J, Kryvi H *et al.* Fecundity, atresia, and egg size of captive Atlantic cod *(Gadus morhua)* in relation to proximate body-composition. *Can J Fish Aquat Sci* 1991;**48**:2333–43. https://doi.org/10.1139/f91-274

Kjesbu OS, Marshall CT, Righton D *et al.* Thermal dynamics of ovarian maturation in Atlantic cod (*Gadus morhua*). *Can J Fish Aquat Sci* 2010;**67**:605–25. https://doi.org/10.1139/F10-011

Kjesbu OS. The spawning activity of cod, *Gadus morhua* L. *J Fish Biol* 1989;**34**:195–206. https://doi.org/10.1111/j.1095-8649.1989.tb03302.x

Kjesbu OS. Time of start of spawning in Atlantic cod (*Gadus morhua*) females in relation to vitellogenic oocyte diameter, temperature, fish length and condition. *J Fish Biol* 1994;**45**:719–35. https://doi.org/10.1111/j.1095-8649.1994.tb00939.x

Krylov VV, Izvekov EI, Pavlova VV *et al.* Circadian rhythms in zebrafish (*Danio rerio*) behaviour and the sources of their variability. *Biol Rev* 2021;**96**:785–97. https://doi.org/10.1111/brv.12678

Kucharczyk D, Czarkowski T, Nowosad J *et al.* Influence of temperature on successful European eel female maturation under controlled conditions. *Turk J Fish Aquat Sci* 2016;**16**:477–82. https://doi.org/10.4194/1303-2712-v16_2_28

Kurita Y, Meier S, Kjesbu OS. Oocyte growth and fecundity regulation by atresia of Atlantic herring (*Clupea harengus*) in relation to body condition throughout the maturation cycle. *J Sea Res* 2003;**49**:203–19. https://doi.org/10.1016/S1385-1101(03)00004-2

Ljubobratovic U, Ardo L, Fazekas G *et al.* Effect of thermal management on vitellogenesis and maturation in indoor-reared pikeperch (*Sander lucioperca*). *Czech J Anim Sci* 2024;**69**:18–28. https://doi.org/10.17221/136/2023-CJAS

Longhurst AR. *Ecological Geography of the Sea*. Burlington, MA: Academic Press, 2007.

Ma Y, Kjesbu OS, Jørgensen T. Effects of ration on the maturation and fecundity in captive Atlantic herring (*Clupea harengus*). *Can J Fish Aquat Sci* 1998;**55**:900–8. https://doi.org/10.1139/f97-305

McQueen K, Marshall CT. Shifts in spawning phenology of cod linked to rising sea temperatures. *ICES J Mar Sci* 2017;**74**:1561–73. https://doi.org/10.1093/icesjms/fsx025

McQueen K, Meager JJ, Nyqvist D *et al.* Spawning Atlantic cod (*Gadus morhua* L.) exposed to noise from seismic airguns do not abandon their spawning site. *ICES J Mar Sci* 2022;**79**:2697–708. https://doi.org/10.1093/icesjms/fsac203

Meek A. The spawning of the cod. Report on the Scientific Investigations. *Northumberland Sea Fisheries Committee*.1911;**1911**:24–5.

Melle W, Runge JA, Head E *et al.* The North Atlantic Ocean as habitat for *Calanus finmarchicus*: environmental factors and life history traits. *Prog Oceanogr* 2014;**129**:244–84. https://doi.org/10.1016/j.pocean.2014.04.026

Morgan MJ, Wright PJ, Rideout RM. Effect of age and temperature on spawning time in two gadoid species. *Fish Res* 2013;**138**:42–51. https://doi.org/10.1016/j.fishres.2012.02.019

Neuheimer AB, MacKenzie BR, Payne MR. Temperature-dependent adaptation allows fish to meet their food across their species' range. *Sci Adv* 2018;**4**:eaar4349. https://doi.org/10.1126/sciadv.aar4349

Neuheimer AB, MacKenzie BR. Explaining life history variation in a changing climate across a species' range. *Ecology* 2014;**95**:3364–75. https://doi.org/10.1890/13-2370.1

Opdal AF, Lindemann C, Fiksen Ø *et al.* Land use change and coastal water darkening drive synchronous dynamics in phytoplankton and fish phenology on centennial time scales. *Glob Chang Biol* 2024a;**30**:17308. https://doi.org/10.1111/gcb.17308

Opdal AF, Wright PJ, Blom G *et al.* Spawning fish maintain trophic synchrony across time and space beyond thermal drivers. *Ecology* 2024b;**105**:e4304. https://doi.org/10.1002/ecy.4304

Óskarsson GJ, Kjesbu OS, Slotte A. Predictions of realised fecundity and spawning time in Norwegian spring-spawning herring (*Clupea harengus*). *J Sea Res* 2002;**48**:59–79. https://doi.org/10.1016/S1385-1101(02)00135-1

Otterå H, Agnalt AL, Jorstad KE. Differences in spawning time of captive Atlantic cod from four regions of Norway, kept under identical conditions. *ICES J Mar Sci* 2006;**63**:216–23. https://doi.org/10.1016/j.icesjms.2005.11.004

Pankhurst NW, Munday PL. Effects of climate change on fish reproduction and early life history stages. *Mar Freshwater Res* 2011;**62**:1015–26. https://doi.org/10.1071/MF10269

Pedersen T. Variation in peak spawning of Arcto-Norwegian cod (*Gadus morhua* L.) during the time period 1929-1982 based on indices estimated from fishery statistics. In: Dahl E, Danielssen DS, Moksness E. et al. (eds), *The Propagation of Cod, Gadus morhua L*. Bergen: Flødevigen Rapportserie, Institute of Marine Research, 1984, 301–16.

Poloczanska ES, Burrows MT, Brown CJ *et al.* Responses of marine organisms to climate change across oceans. *Front Mar Sci* 2016;**3**:62. https://doi.org/10.3389/fmars.2016.00062

Qasim SZ. Time and duration of the spawning season in some marine teleosts in relation to their distribution. *ICES J Mar Sci* 1956;**21**:144–55. https://doi.org/10.1093/icesjms/21.2.144

Rogers LA, Dougherty AB. Effects of climate and demography on reproductive phenology of a harvested marine fish population. *Glob Chang Biol* 2019;**25**:708–20. https://doi.org/10.1111/gcb.14483

Samplonius JM, Atkinson A, Hassall C *et al.* Strengthening the evidence base for temperature-mediated phenological asynchrony and its impacts. *Nat Ecol Evol* 2021;**5**:155–64. https://doi.org/10.1038/s41559-020-01357-0

Santos AMP, Re P, Dos Santos A *et al.* Vertical distribution of the European sardine (*Sardina pilchardus*) larvae and its implications for their survival. *J Plankton Res* 2006;**28**:523–32. https://doi.org/10.1093/plankt/fbi137

Schneider CA, Rasband WS, Eliceiri KW. NIH image to ImageJ: 25 years of image analysis. *Nat Methods* 2012;**9**:671–5. https://doi.org/10.1038/nmeth.2089

Skjæraasen JE, Karlsen O, Langangen O *et al.* Impact of salmon farming on Atlantic cod spatio-temporal reproductive dynamics. *Aquacult Env Interact* 2021;**13**:399–412. https://doi.org/10.3354/aei00415

Skjærven KH, Alix M, Kleppe L *et al.* Ocean warming shapes embryonic developmental prospects of the next generation in Atlantic cod. *ICES J Mar Sci* 2024;**81**:733–47. https://doi.org/10.1093/icesjms/fsae025

Sokal RR, Rohlf FJ. *Biometry: the Principles and Practice of Statistics in Biological Research*.New York:Freeman, 2012.

Sverdrup HU, Johnson MW, Fleming RH. *The Oceans. Their Physics, Chemistry and General Biology*. New York:Prentice-Hall, Inc, 1942.

Sverdrup HU. On conditions for the vernal blooming of phytoplankton. *J Cons* 1953;**18**:287–95. https://doi.org/10.1093/icesjms/18.3.287

Tanaka H, Nakagawa T, Yokota T *et al.* Effects of spawning temperature on the reproductive characteristics of walleye pollock *Gadus chalcogrammus*. *Fish Sci* 2019;**85**:901–11. https://doi.org/10.1007/s12562-019-01343-x

Thorsen A, Kjesbu OS. A rapid method for estimation of oocyte size and potential fecundity in Atlantic cod using a computer-aided particle analysis system. *J Sea Res* 2001;**46**:295–308. https://doi.org/10.1016/S1385-1101(01)00090-9

Ware DM, Tanasichuk RW. Biological basis of maturation and spawning waves in Pacific herring (*Clupea harengus pallasi*). *Can J Fish Aquat Sci* 1989;**46**:1776–84. https://doi.org/10.1139/f89-225

Wieland K, Jarre-Teichmann A, Horbowa K. Changes in the timing of spawning of Baltic cod: possible causes and implications for recruitment. *ICES J Mar Sci* 2000;**57**:452–64. https://doi.org/10.1006/jmsc.1999.0522

Witthames PR, Greer Walker M. Determinacy of fecundity and oocyte atresia in sole (*Solea solea*) from the Channel, the North Sea and the Irish Sea. *Aquat Living Resour* 1995;**8**:91–109. https://doi.org/10.1051/alr:1995007

Witthames PR, Thorsen A, Murua H *et al.* Advances in methods for determining fecundity: application of the new methods to some marine fishes. *Fish Bull* 2009;**107**:148–64.

Wood SN. *Generalized Additive Models: an Introduction with R*. New York: Chapman and Hall/CRC, 2017,496. https://doi.org/10.1201/9781315370279

Woodhead AD, Woodhead PMJ. Seasonal changes in the physiology of the Barents Sea cod, *Gadus Morhua* L., in relation to its environment. *ICNAF Environmental Symposium 1964, Special Publication*, 1966;6;691–715. https://www.nafo.int/Portals/0/PDFs/icnaf/Special-pub/special-pub-6secF.pdf

Wright PJ, Orpwood JE, Boulcott P. Warming delays ovarian development in a capital breeder. *Mar Biol* 2017;**164**;article no 80.

Yoneda M, Wright PJ. Effects of varying temperature and food availability on growth and reproduction in first-time spawning female Atlantic cod. *J Fish Biol* 2005;**67**:1225–41. https://doi.org/10.1111/j.1095-8649.2005.00819.x

Handling editor: Dominique Robert

Received: 10 November 2025. **Revised:** 30 January 2026. **Accepted:** 30 January 2026